

The Effect of Surface Induced Flows on Bubble and Particle Aggregation

Scott A. Guelcher, Yuri E. Solomentsev, Marcel Böhmer*, John L. Anderson, and Paul J. Sides**

Department of Chemical Engineering
Carnegie Mellon University
Pittsburgh, PA 15213

*Philips Research Laboratories
Eindhoven, Prof. Holstlaan 4
5656 AA Eindhoven, The Netherlands

**Corresponding author: ps7r@andrew.cmu.edu

ABSTRACT

Almost 20 years have elapsed since a phenomenon called "radial specific coalescence" was identified. During studies of electrolytic oxygen evolution from the back side of a vertically oriented, transparent tin oxide electrode in alkaline electrolyte, one of the authors (Sides) observed that large "collector" bubbles appeared to attract smaller bubbles. The bubbles moved parallel to the surface of the electrode, while the electric field was normal to the electrode surface. The phenomenon was reported but not explained. More recently self ordering of latex particles was observed during electrophoretic deposition at low DC voltages likewise on a transparent tin oxide electrode. As in the bubble work, the field was normal to the electrode while the particles moved parallel to it. Fluid convection caused by surface induced flows (SIF) can explain these two apparently different experimental observations: the aggregation of particles on an electrode during electrophoretic deposition, and a radial bubble coalescence pattern on an electrode during electrolytic gas evolution. An externally imposed driving force (the gradient of electrical potential or temperature), interacting with the surface of particles or bubbles very near a planar conducting surface, drives the convection of fluid that causes particles and bubbles to approach each other on the electrode.

Phenomena. Two seemingly different phenomena, the aggregation of colloidal particles deposited on an electrode and the coalescence of gas bubbles generated near an electrode, can be explained from a unified point of view based on considering fluid convection. Sides and Tobias^{1,2} studied the electrolytic evolution of oxygen bubbles from the back side of a vertically oriented, transparent tin oxide electrode in alkaline electrolyte. The authors

discovered a phenomenon they termed "specific radial coalescence," whereby central "collector" bubbles appeared to attract smaller bubbles. A sequence of images from these experiments, appearing in Figure 1, demonstrates the effect.² The first frame shows a large bubble in the lower left quadrant with six smaller bubbles arranged around it in a near hexagonal array. As time elapses, each smaller bubble moves toward the large bubble until it eventually coalesces with it. The bubbles move as if "attracted" to the larger bubble from all points surrounding it; the effect was therefore independent of gravity since buoyancy would have moved the bubbles unidirectionally. Most of the bubbles in the experiment were mobile, which indicates the presence of a small but finite film of liquid between the bubbles and the electrode. Janssen and van Stralen³ reported similar observations of lateral bubble motion on a transparent electrode during electrolytic gas evolution. The interactions between the bubbles appeared to be significant over distances over several bubble diameters (tens of microns) and could not be attributed to conventional colloidal/surface forces.

Colloidal particles can form ordered layers in both direct and alternating electric fields during electrophoretic deposition (EPD) on conducting surfaces.^{5,6,7,8} Conditions under which the self-ordering occurs vary widely. Böhmer⁴, studying field-induced lateral motion of 4 and 10 μm polystyrene spheres on a transparent indium-doped tin oxide (ITO) electrode, observed *in situ* clustering under direct current field strengths less than 20 V/m. The particles on the surface of the electrode aggregated to form clusters even though the particles were initially several radii apart. A time series of photographs, appearing in Figure 2, demonstrates this field-induced cluster formation. The first

doublets formed after 60 s. (Figure 2b). Subsequently, these doublets formed triplets and higher-order aggregates (Figure 2b, 2c). Particle-cluster and cluster-cluster aggregation continued until, as seen in the last picture of the series taken after 12 minutes, only one particle was left and several large ordered clusters were formed (Figure 2f). This series of photographs shows both the long-range nature of the interactions and cluster-cluster aggregation. The clusters separated into single particles when the electric field was reversed. Also, the particles exhibited Brownian motion even when they appeared to be on the surface of the electrode, which again indicated the presence of a small but finite gap of liquid between the particles and the electrode.

We propose a unified explanation for self-aggregation of particles and bubbles near surfaces. The mechanism is based on convection induced by the surfaces of particles or bubbles as they interact with an electric field or temperature gradient normal to the surface. Gradients perpendicular to fluid/fluid interfaces are known to produce convection^{9,10,11}, but these flows originate from perturbations in the interfacial tension caused by the coupling of electrical, thermal and composition gradients with deformation of the interface. The foundation of this model, however, is *steady* convection resulting from flows about particles and bubbles held stationary at a solid surface. The analysis for particle clustering is an elaboration of the mechanism first proposed by Böhmer⁴.

Analysis. We attribute the long-range interactions (of several radii) between particles and bubbles near a conducting solid-liquid interface to fluid convection induced by interactions between the applied field (electrical or thermal) and the surface of the particles and bubbles. These phoretic interactions¹² create a recirculating fluid flow pattern in the vicinity of the bodies. For a particle near an electrode, the electrical stresses resulting from the action of the electric field on the ions within the electrical double layer about the particle's surface produce an electroosmotic "slip velocity" at the outer edge of the double layer that drives the flow about the particle as shown in Figure 3a. The slip velocity is given by the Helmholtz expression, $\mathbf{v}^s = (-\epsilon \zeta / \eta) \mathbf{E}$, where ϵ is the permittivity of the fluid (water), η is the viscosity, ζ is the zeta potential of the particle's surface¹³, and \mathbf{E} is the electric field tangent to the particle's surface.

For a bubble near a heated wall, an interfacial tension gradient over the bubble's surface results from an overall temperature gradient perpendicular to the wall. Fluid flow must balance the resulting interfacial stress at the interface, $\sigma^s = \gamma' \nabla T$ where γ' is the derivative of interfacial tension with temperature and ∇T is the temperature gradient at the interface.^{14,15} Calculated fluid streamlines for this type of "Marangoni" flow appear in Figure 3b.

The phoretic velocity fields about a particle or bubble held stationary very near a planar electrode must be calculated in order to compare our hydrodynamic theory quantitatively with experimental observations of aggregation. For the case of a non-conducting, charged, spherical particle that is large relative to the thickness of the double layer, we first determined the spatial variation of the electrical potential by solving Laplace's equation which follows from charge (ion) conservation in the electrolyte solution. The potential on the electrode was assumed uniform. From this solution we calculated the electric field \mathbf{E} at each point on the surface of the particle, from which the slip velocity was determined. Then the steady Stokes-flow equations were solved using the slip velocity boundary condition ($\mathbf{v} = \mathbf{v}^s$) at the particle's surface (*i.e.*, at the outer edge of the double layer). Details are given by Solomentsev *et al.*¹⁶ The streamlines of Figure 3a are essentially the same for any gap distance h less than 10% of the radius of the particle. The calculation of the Marangoni flow field in the vicinity of a bubble very near a heated plane wall at uniform temperature proceeded similarly except that the Stokes equations were solved by balancing the hydrodynamic stress with the interfacial stress ($\sigma = \sigma^s$) at the surface of the bubble. The overall thermal gradient, used as the boundary condition far from the bubble, was calculated from the heat dissipation on the electrode's surface due to electrochemical reaction on the electrode and ohmic heat production in the antimony-doped tin oxide film, as described later. Again, the streamlines of Figure 3b are independent of the gap between the bubble and the surface when it is less than 10% of the particle's radius.

The calculated streamlines for either electroosmotic or Marangoni flows, Figure 3, indicate that the effect of convection could be to either attract two particles or repel them. A "test" body adjacent to the electrode will be convected toward the first body. The flow field about the test body will have a similar effect on the first body if they are of equal

size, so that the two particles or bubbles approach each other. A test body far from the electrode will be convected away from the first body as it approaches the electrode but then will be convected toward the first body when it is near the electrode. Since the flow is linear with the applied electric or temperature field, the direction of the fluid velocity changes if the direction of the field is reversed, which resulted in the de-clustering of particles observed experimentally⁵ in the case of electrophoretic deposition.

In the case of EPD of particles, we have analyzed the clustering of groups of particles by neglecting the effects of multiple particles on the local electrical potential and fluid velocity. The velocity of a test particle toward the central particle, v_r , is assumed equal to the fluid velocity in the absence of the test particle, v_{r0} , multiplied by a correction factor q to account for the hydrodynamic hindrance due to the electrode surface.¹⁷ Multiple simulations of triplets of different initial configurations accounted for the random nature of the aggregation process. The initial configuration of the three particles was chosen randomly except that no overlap was allowed. The position versus time of each particle was computed by integrating its velocity over time, where the particle's velocity was given by the sum of v_r caused by the other two particles. The parameter q was considered a single adjustable parameter independent of the relative positions of the three particles.¹⁶ Details of the calculations are reported elsewhere.

The de-clustering time of a triplet (T^E), defined as the time required for the three initially contiguous particles to disaggregate, was calculated as a function of the final mean center-to-center separation distance ($d = [d_{12} + d_{13} + d_{32}]/3$) between the particles for random initial configurations. The following expression approximates the calculated values of $T^E(d)$ in the range $2 < d < 7$ very well:

$$T^E(d) = 2.19 \frac{(d-2)}{q} \exp(0.277d) \quad (1)$$

This theoretical result is compared to the experimental data of Böhmer⁵ in Figure 4. The experimental data are for de-clustering of triplets upon reversal of the field; thus, d represents the mean spacing at each time. In this plot, the separation distance was normalized by the particle's radius (a), and the de-clustering time by a/v^s with $|E|$ equal to the applied electric field perpendicular to

the electrode. The best-fit value of the hydrodynamic correction factor (q) is 0.5, which is expected for gaps between the particle and electrode of 1-10% of the particle's radius.

Symbols of different shapes in Figure 4 represent different triplets in the experiments. The applied voltage was different for each triplet, either -1 V or -1.5 V. The data as plotted in Figure 4, with time normalized by the slip velocity v^s (which is itself proportional to the applied electric field), indicate that the relative motion among the three particles was linear with the electric field, as predicted by the theory.

Although the liquid-gas interface might be charged, the motion of bubbles at electrodes leading to specific radial coalescence cannot be attributed to electroosmosis because the velocities observed by Sides and Tobias⁷ were two to three orders of magnitude higher than the estimated magnitude of the electroosmotic slip velocity v^s . On the other hand, the observed lateral motion of equal-size bubbles toward each other can be explained in terms of Marangoni convection around each bubble near the electrode, where the velocity scale is given by $v^m = g' - Ta/2h$ with g' being the derivative of surface tension with respect to temperature and a the bubble's radius.¹⁵ The theory for this case resembles the theory developed for deposited particles; that is, a test bubble is entrained in the convective flow about the other bubble (v_{r0}) and moves toward it at velocity $v_r = qv_{r0}$ where q is the hindrance factor of the electrode. These calculations for the change in center-to-center distance (d) between the bubbles as a function of time (t) are fit by the following empirical equation ($h=0.05$):

$$d(t) = q(3.336 - 0.185t)\exp(0.030t) \quad (2)$$

The distance is normalized by a and the time by a/v^m .

The temperature gradient at the surface of the bubble must be determined in order to calculate the magnitude of the Marangoni flow field about a deposited bubble. We solved Laplace's equation for the temperature field around a bubble subject to a constant uniform temperature at the electrode and a specified gradient of temperature far from the bubble and the electrode. In the experiments of Sides and Tobias, no temperature measurements were made, so the far-field gradient was estimated from the irreversibilities of the electrochemical reaction and

the ohmic losses in the thin tin oxide electrode used in the experiments. The homogeneous ohmic heating of the electrolyte was neglected in these calculations because it raised the overall temperature but did not affect the gradients on the time scale of the experiments. We used film theory¹⁸ in the aqueous phase to express this gradient $(-T)_0 = Q/k$, where Q is the heat flux dissipated from the electrode, and k is the thermal conductivity of the electrolyte. This quotient is a reasonable approximation of the average gradient for bubbles having diameters smaller than the thermal boundary layer thickness. Estimating the thickness of the thermal boundary layer by analogy from mass transfer correlations developed for electrolytic gas evolution⁹, one obtains approximately 140 μm , which is between three and four times the diameter of the largest bubble considered in this analysis. Prior analysis has shown that this distance from the electrode is sufficient for disturbances in the potential or the temperature to relax.²⁰ The heat flux Q from the anode to the electrolyte can be approximated by the sum of the irreversible heat flux Q_{rxn} generated at the anode surface by the electrode reaction, and the ohmic heat flux from the tin oxide film Q_{film} . The flux Q_{rxn} is calculated by

$$Q_{\text{rxn}} = i \eta_{\text{rxn}} \quad (3)$$

where i is the current density and η_{rxn} is the electrochemical overpotential for oxygen evolution. The ohmic heat flux is calculated by

$$Q_{\text{film}} = i^2 R_{\text{sq}} L^2 \quad (4)$$

where L is the effective current path length taken as half the cell width (1.5×10^{-3} m). The electrode had an electrical resistivity $R_{\text{sq}} = 100$ ohms per square. For a current density of $5,000 \text{ A m}^{-2}$ and an overpotential of 1 V, the above equations yield a total heat flux $Q = 10,600 \text{ W m}^{-2}$ and a temperature gradient $(-T)_0 = 17,700 \text{ K m}^{-1}$; for a current density of $1,000 \text{ A m}^{-2}$, the temperature gradient was $2,070 \text{ K m}^{-1}$. The bubbles ranged in radius from 13 to 22 μm . Therefore, we estimate that the temperature difference between the bottom (hot region) and top (cold region) of the bubbles varied from about 0.05 K to 0.8 K. The corresponding difference in interfacial tension varied from about $0.007 \times 10^{-3} \text{ N m}^{-1}$ to $0.12 \times 10^{-3} \text{ N m}^{-1}$.

Using the above estimates of the temperature gradient, the theory expressed by equation (2) is

compared to the experimental values of d versus t for four different pairs of bubbles in Figure 5. The data were obtained by analyzing movies of the radial coalescence.⁶ As in the case of particles, there is good agreement between the theory and the experiment, and the data scale as predicted with two different parameters, bubble radius and current density (*i.e.*, temperature gradient). The value of the hydrodynamic correction factor (q) was assumed to be 1.0.

Discussion Aggregation of particles near an electrode and coalescence of bubbles near a heated wall are physically different phenomena but can be explained by a similar hydrodynamic mechanism resulting from convection induced by interfacial forces. For bodies of approximately the same size, the phoretic flow theory is in reasonable agreement with the experimental data when the hydrodynamic correction factor q is of order unity. The analysis described above accounts for the aggregation of equal-size particles or bubbles (Figure 1), but modification of the theory is necessary when the primary particle is much larger than the test particle (Figure 2). In this case the velocity of the test particle (bubble) toward the primary particle (bubble) is a superposition of the mutual entrainment mechanism described in this paper and the additional electrophoretic (thermocapillary) velocity caused by perturbation of the electrical potential (temperature) around the primary particle (bubble). For a size ratio of about 0.2, the attractive velocity due to the perturbed electrical potential is comparable to the convective velocity; thus, the velocity of a small particle in close proximity of a large collector particle on an electrode can be significantly greater than the entrainment velocity of a particle of the same size as the collector particle.

Yeh *et al.*⁶ observed clustering under conditions of alternating current (1 kHz) and a field strength of 25,000 V/m. These authors offered a qualitative explanation based on electrohydrodynamic interaction of lateral electric field gradients with the double layer of the electrode rather than the particle. Their model does not predict sufficient flow velocities at the field strengths used by Böhmer to explain his observations. Furthermore, Yeh *et al.*'s model cannot explain the motion of bubbles on electrodes mentioned above. To compare the expected flow velocities predicted by the model of Yeh *et al.* and the results reported herein under Böhmer's conditions, we calculated the ratio of the lateral fluid velocities predicted by the two models. Assuming that within the electrode double layer current is carried by a single ionic species of

concentration n_0 , Yeh *et al.* presented the following equation for the transverse fluid velocity v_t :

$$v_t \approx \frac{k_B T}{\eta D_0} \frac{l_d^3 J_0}{eR} \quad (5)$$

where k_B is the Boltzmann constant, e is electron charge, D_0 is the diffusion coefficient of the ion, l_d is the double layer thickness, J_0 is the current density, and R is the length scale of the feature on the electrode surface. Since the feature on the electrode in the present case is a particle, R is the particle radius. The fluid velocity due to electroosmosis v_{eo} about a deposited charged particle, according to our model, is:

$$v_{eo} = f(r) \frac{\epsilon \zeta}{\eta} E_\infty \quad (6)$$

where E_∞ is the magnitude of the applied electric field and $f(r)$ is a factor less than unity that gives the correct estimation of the transverse flow as a function of center-to-center distance " r ". The ratio v_{eo}/v_t is calculated from the following equation:

$$\frac{v_{eo}}{v_t} = f(r) \frac{e}{k_B T} \frac{\epsilon \zeta a D_0}{\kappa l_d^3} \quad (7)$$

where κ is the specific conductivity of the electrolyte. Values of v_{eo}/v_t as a function of the center-to-center distance r between two particles on the surface of the electrode are presented in Table 1. The data indicate that the electroosmotic phenomenon described in this work is 1 to 2 orders of magnitude stronger than the effect described by Yeh *et al.* for the conditions of Böhmer's experiments.

Our conclusion is that a purely hydrodynamic model for self-aggregation of nearly equal-size particles deposited on an electrode and for bubbles formed on a hot surface (which here is an electrode) can quantitatively explain the observed rates of clustering and coalescence. The concept is that the fluid convection driving aggregation derives from direct interactions between the field (electrical or thermal) and the deposited species (particle or bubble).

Acknowledgments This work was partially supported under NSF Grant CTS-9420780. S.G. acknowledges support from the NASA Graduate Student Researchers Program under Grant NGT5-50054.

References

1. Sides, P. J. Bubble Dynamics at Gas Evolving Electrodes, Ph.D. Thesis, University of California, Berkeley, 1981.
2. Sides, P.J. & Tobias, C.W. *J. Electrochem. Soc.* **132**, 583 (1985).
3. Janssen, L.J.J. & van Stralen, S.J.D. *Electrochimica Acta* **26**, 1011 (1981).
4. Böhmer, M. *Langmuir* **12**, 5747 (1996).
5. Trau, M., Saville, D.A. & Aksay, I.A. *Science* **272**, 706 (1996).
6. Yeh, S.-R., Seul, M. & Shraiman, B.I. *Nature* **386**, 57 (1997).
7. Giersig, M. & Mulvaney, P. *J. Phys. Chem.* **97**, 6334 (1993).
8. Giersig, M. & Mulvaney, P. *Langmuir* **9**, 3408 (1993).
9. Taylor, G.I. & McEwan, A.D. *J. Fluid Mech* **22**, 1 (1965).
10. Sterling, C.V. & Scriven, L.E. *AIChE J.* **5**, 514 (1959).
11. Scriven, L.E. & Sterling, C.V. *Nature* **187**, 186 (1960).
12. Anderson, J.L. *Annual. Rev. Fluid Mech.* **21**, 61 (1989).
13. Hunter R.J., Zeta potential in colloid science : principles and applications. London: Academic Press, 386 (1981).
14. Levich, V.G. & Krylov, V.S. *Annual Rev. Fluid Mech.* **1**, 293 (1969).
15. Young, N.O., Goldstein, J.S & Block, M.J. *J. Fluid Mech.* **6**, 350 (1959).
16. Solomentsev, Yu., Böhmer, M. & Anderson, J.L. submitted to *Langmuir* (1997).
17. Goldman, A.J., Cox, R.G. & Brenner, H. *Chem. Eng. Sci.* **22**, 653 (1967).
18. Bird, R.B., Stewart, W.E. & Lightfoot, E.N., Transport Phenomena. New York: John Wiley & Sons, 659 (1960).
19. Sides, P. J., "Phenomena and Effects of Electrolytic Gas Evolution" *Modern Aspects of Electrochemistry* V. **18** R. E. White, B. E. Conway, J. O'M. Bockris, eds., Plenum, New York (1986).
20. Sides, P. J. and C.W. Tobias, *Journal of the Electrochemical Society* **127**, 288 (1980).

Figure Captions

Figure 1. Frames from the movie of Sides and Tobias showing electrolytic gas evolution (oxygen) from the back side of a tin oxide electrode in KOH. The bubbles grow away from the viewer as if on the far side of a pane of glass. The frames represent a square about 150 mm on a side and approximately 0.4 ms elapses between frames. One can particularly see the phenomenon of specific radial coalescence by following the fates of bubbles 1 - 6 as they seem to be attracted to the larger bubble they surround. Bubbles 7 and 8 will coalesce with the bubble on the right edge of the viewing area.

Frame 4: Bubble 1 has arrived at its "collector" bubble and coalesces with it in frame 5. Bubbles 2-5 are approaching their collector bubble. Bubble 8 reaches the bubble on the right edge of the frame (left) and coalesces with it in frame 5. Bubble 7 is moving toward the bubble on the right edge.

Frame 7: Bubbles 2 - 5 have all reached the collector. Bubble 8 has reached its collector.

Frame 9: All bubbles have coalesced with their respective collectors..

Figure 2. Time series for the formation of clusters of 10 μm PS particles starting from a semi-regular array at 1.5 V.

Figure 3. a) Fluid convection induced by electroosmosis about a stationary particle near an electrode whose surface is the horizontal axis at the bottom. In this example the particle could be negative and the electrode positive, so the electroosmotic slip velocity draws fluid upward near the particle. If the particle and electrode have the same sign of charge, then the arrows on the streamlines are reversed. The fluid velocity is zero along the electrode's surface. b) Convection induced by thermocapillary motion about a stationary bubble near a surface where a uniform gradient of temperature exists perpendicular to the surface, such that the surface is hotter than the fluid. If the temperature gradient is reversed, then the arrows on the streamlines are reversed.

Figure 4. De-clustering time as a function of the mean center-to-center distance d for three particles. Time is normalized by a/v_s where a is the particle's radius and v_s is the magnitude of the electroosmotic slip velocity ($= (ez/h)E_0$), while the separation distance is normalized by a . The symbols are the data from the experiments by Böhmer³ in which three particles initially in contact separated (de-clustered) when the electric field was reversed; in this case, d is the mean separation among the three particles at the designated time. Each symbol represents a different triplet, and the horizontal error bars correspond to the standard deviations of the distance measurements. The solid line is the prediction from the hydrodynamic theory (equation (1)) with the hydrodynamic hindrance factor $q = 0.50$. For the theoretical predictions, d is the initial mean separation and the vertical bars are the standard deviations of simulations for the range $2 < d < 5$ (10-15 trials at each separation), with random but non-overlapping initial placement of the three particles.

Figure 5. Dimensionless center-to-center distance d as a function of dimensionless time t for 8 pairs of bubbles of approximately equal size. The parameter t is normalized by a/v_m where v_m is the magnitude of the Marangoni velocity ($v_m = g' - \Delta T a / 2h$), and d is normalized by the particle's radius a . Filled symbols correspond to a current density of 1000 A m^{-2} , while the open symbols correspond to a current density of 5000 A m^{-2} . Symbols of different shapes represent different pairs of bubbles. The solid line is calculated from the theory (equation (2)) with $q = 1.0$.

Table 1

Center-to-center distance (radii)	$f(r)$	v_{e0}/v_t
4	0.06	31
3	0.12	63
2	0.18	94

Ratio of the expected electroosmotic velocity v_{e0} to the transverse electrohydrodynamic velocity v_t of Yeh *et al.* calculated from eq (7). The calculations were performed based on the experimental conditions of Böhmer: ion concentration $n_0 = 10^{-4}$ M (corresponding to $l_d = 30 \cdot 10^{-9}$ m and $\kappa = 15 \cdot 10^{-4}$ ohm $^{-1}$ m $^{-1}$), ionic diffusion coefficient $D_0 = 2 \cdot 10^{-9}$ m 2 s $^{-1}$, particle zeta potential $\zeta = 0.08$ V, and particle radius $a = 5 \cdot 10^{-6}$ m.

Figures

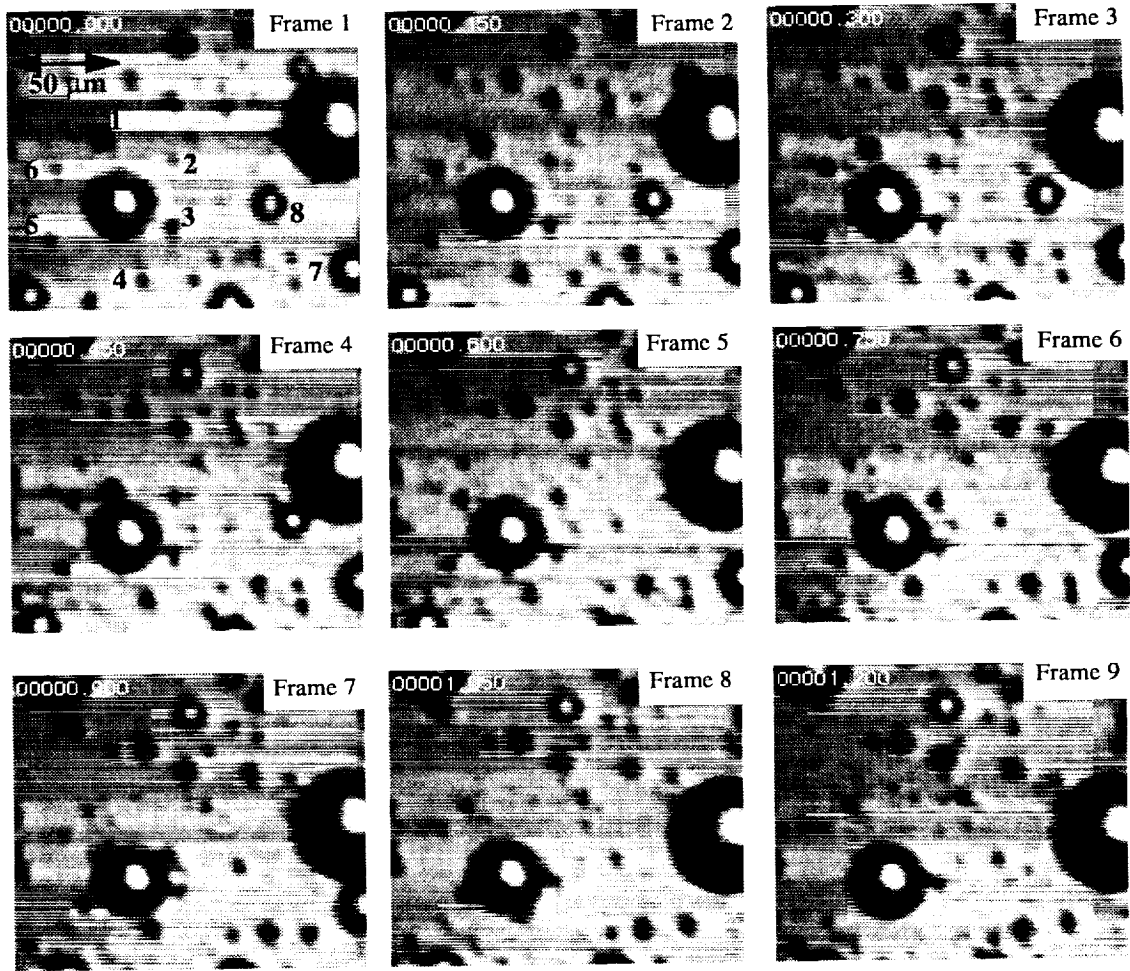
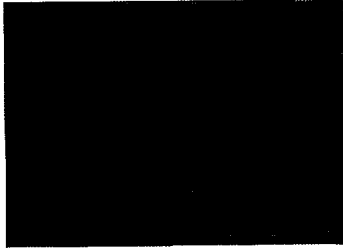
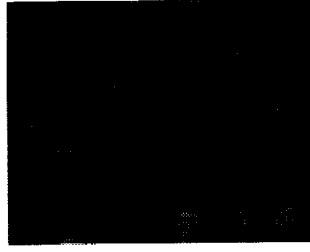


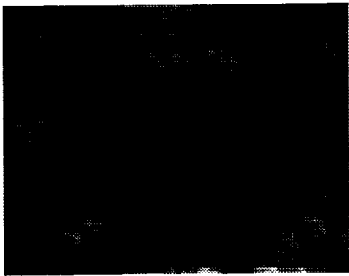
Figure 1.



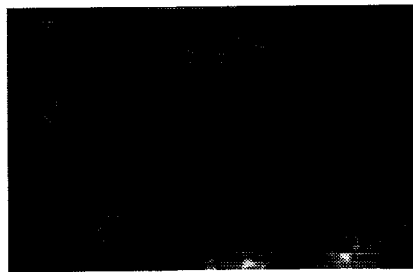
a.



b.

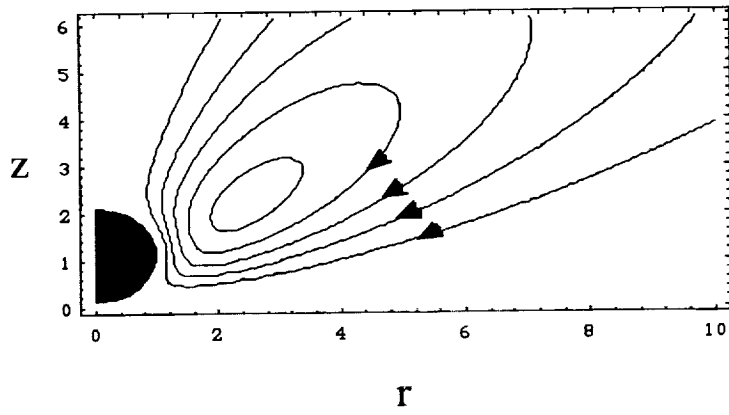


c.

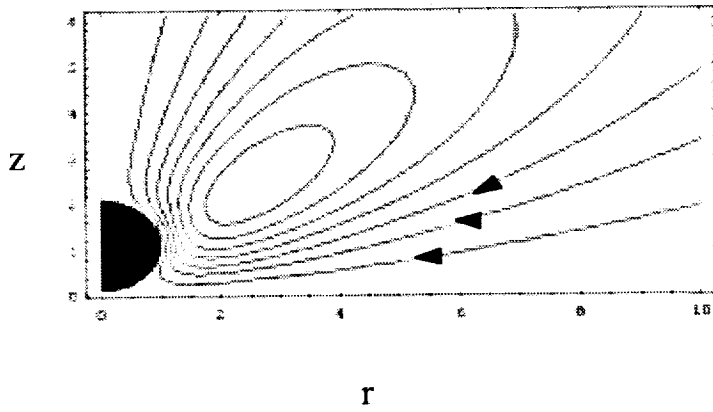


d.

Figure 2.



a.



b.

Figure 3.

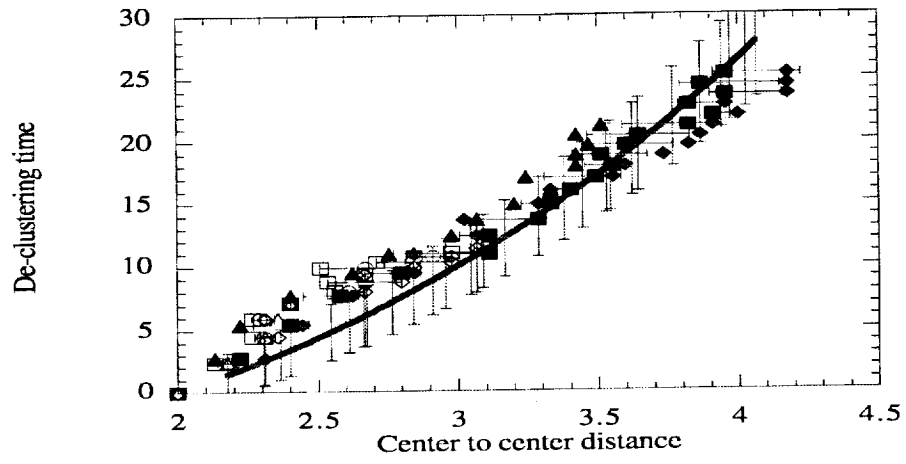


Figure 4.

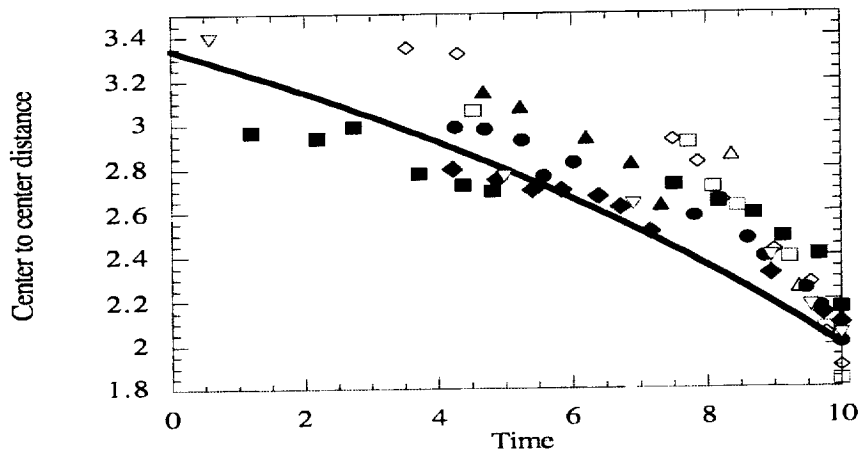


Figure 5.